

Non-Intrusive Load Monitoring with an Attention-based Deep Neural Network

¹Antonio Maria Sudoso and ¹Veronica Piccialli

¹Department of Civil and Computer Engineering, University of Rome Tor Vergata, Rome, IT

Abstract—Energy disaggregation, also referred to as a Non-Intrusive Load Monitoring (NILM), is the task of using an aggregate energy signal, for example coming from a whole-home power monitor, to make inferences about the different individual loads of the system. In this paper, we present a novel approach based on the encoder-decoder deep learning framework with an attention mechanism for solving NILM. The attention mechanism is inspired by the temporal attention mechanism that has been recently applied to get state-of-the-art results in neural machine translation, text summarization and speech recognition. The experiments have been conducted on two publicly available datasets AMPds and UK-DALE in seen and unseen conditions. The results show that our proposed deep neural network outperforms the state-of-the-art Denoising Auto-Encoder (DAE) proposed initially by Kelly and Knottenbely (2015) and its extended and improved architecture by Bonfigli et al. (2018), in all the addressed experimental conditions. We also show that modeling attention translates into the ability to correctly detect the state change of each appliance, that is of extreme interest in the field of energy disaggregation.

Index Terms—Attention Mechanism, Deep Neural Network, Energy Disaggregation, Non-Intrusive Load Monitoring.

I. INTRODUCTION

Non-Intrusive Load Monitoring (NILM) is the task of estimating the power demand of each appliance given aggregate power demand signal recorded by a single electric meter monitoring multiple appliances [1]. In the last years, the research on NILM has been particularly active in the field of machine learning. In the literature, solutions based on Support Vector Machine (SVM), Nearest Neighbour (k-NN) and different variants of Hidden Markov Models (HMMs) have been proposed [2]. Among these techniques, approaches based on deep learning have received particular attention since they exhibited noteworthy disaggregation performance. Inspired by the success of Deep Neural Networks (DNNs) in the fields of computer vision, audio and natural language processing, DNNs have been successfully applied for the first time to NILM by Kelly & Knottenbely in [3], which coined the term ‘Neural NILM’. Neural NILM is sequence-to-sequence regression problem that consists of training a neural network for each appliance in order to predict a time window of the disaggregate active power from a time window of aggregated data. Kelly & Knottenbely proposed three different neural network architectures to perform NILM with high-frequency time series data: a recurrent neural network (RNN) using Long Short-Term Memory units (LSTM), a Denoising Auto-Encoder (DAE), and a regression model that predicts the start time, end time and average power demand of each appliance. The

capability of LSTMs to successfully learn on data with long range temporal dependencies makes it a natural choice for NILM. For this reason, their first approach is based on stacked layers of LSTM units combined with a Convolutional Neural Network (CNN) at the input of the network to automatically extract features from the raw data. In the same paper, NILM is treated as a noise reduction problem, in which the clean signal is represented by the disaggregated appliance profile and the aggregated signal is assumed corrupted by the presence of the remaining profiles and the measurement noise. For this purpose, noise reduction is performed by means of a DAE composed by convolutional layers and fully connected layers. The experiments conducted by the authors on the UK recording Domestic Appliance-Level Electricity dataset (UK-DALE) [4] demonstrated that the best performing approach is represented by the DAE network that outperforms the other DNN architectures and other approaches frequently employed for this problem such as HMMs and Combinatorial Optimization (CO). In [5], an empirical investigation of deep learning methods is conducted by using two types of neural network architectures for NILM. The first neural network solves a regression problem in which estimates the transient power demand of a single appliance given the whole series of the aggregate power. The second type of network is a multi-layer RNN using LSTM units, which is similar to the structure used in [3]. Zhang et al. in [6] proposed instead a sequence-to-point learning for energy disaggregation in which a single-midpoint of an appliance window is treated as classification output of a neural network with the aggregate window being the input. In [7], Bonfigli et al. proposed several algorithmic and architecture improvements to the DAE for NILM and showed that the Neural NILM approach is able to outperform state-of-the-art NILM approaches which are not based on DNNs like Additive Factorial Approximate Maximum A Posteriori estimation (AFAMAP) by Kolter and Jaakkola [8]. Compared to [3], their DAE approach for load disaggregation is improved by introducing pooling and upsampling hidden layers in the architecture and a median filter in the disaggregation phase to reconstruct the output signal from the overlapped portions of the disaggregated signal.

In this paper, we propose a sequence-to-sequence model with an attention mechanism and we borrow the idea from research papers where this framework has recently given state-of-the-art results for machine translation [9], image captioning [10] and speech recognition [11]. The attention mechanism has the function to locate a set of positions where relevant information is present in the input sequence for generating

the next time step of the target sequence. The intuition is that an attention-based model could help the energy disaggregation task by assigning importance to each position of the aggregated signal which corresponds to the position of a state change of the target appliance. This allows the neural network to focus its representational power on selected time steps of the target appliance in the aggregated signal.

The evaluation of the proposed algorithm is conducted on two publicly available datasets AMPds [12] and UK-DALE, and the performance are evaluated using different metrics. The obtained results show that our algorithm outperforms the state-of-the-art improved DAE proposed by Bonfigli et al. [7] in all the addressed experimental conditions. The paper is organized as follows. Section 2 describes the NILM problem. Section 3 presents our deep neural network architecture. Sections 4 describes the experimental procedure and the obtained results. Finally, Section 5 concludes the paper.

II. NILM PROBLEM

Given a sequence of aggregate power consumption $\{x(t)\}$ from N active appliances at the entry point of the meter at $t = \{1, \dots, T\}$, the task of the NILM algorithm is to infer the power contribution $\{y_i(t)\}$ of appliance $i \in \{1, \dots, N\}$ at time t , such that at any point in time t , the aggregate power consumption is given by the sum of the power consumption of all the known appliances plus a noise term. The energy disaggregation problem can be formally formulated as follows:

$$x(t) = \sum_{i=1}^N y_i(t) + e(t),$$

where $x(t)$ is the aggregated active power measured at time t , $y_i(t)$ is the individual contribution of appliance i , N is the number of appliances, and $e(t)$ is a noise term. In a *denoised* scenario, the noise term is zero, while in a *noised* scenario, it represents the total contribution from appliances not included and the measurement noise. The NILM problem is, thus, the task of estimating the individual appliance contributions $y_i(t)$ given only the aggregated active power measurement $x(t)$. Similarly to [3], we refer to the power over a complete cycle of an appliance as an ‘appliance activation’. The duration of an appliance activation is used to determine the size of the sliding window that selects the input and the output sequences for the Neural NILM modeling.

III. ENCODER-DECODER WITH ATTENTION MECHANISM

This section describes the new deep architecture we have introduced to solve the sequence-to-sequence NILM problem. The network is constituted by three components:

- 1) An encoder, that extracts the set of feature maps and learns a compact representation of the input sequence.
- 2) An attention mechanism, which selects the most significant elements of the sequence correlated to the state changes in the appliance.
- 3) A decoder that reconstructs the disaggregated signal and produces the output sequence.

In the next two subsections we describe the attention mechanism and the network topology in detail.

A. Attention Mechanism

In the classical setting, a sequence-to-sequence network is a model consisting of two components called the encoder and decoder [13]. The encoder is an RNN that takes an input sequence of vectors (x_1, x_2, \dots, x_T) , where T is the length of input sequence, and encodes the information into fixed length vectors (h_1, h_2, \dots, h_T) . This representation is expected to be a good summary of the entire input sequence. The decoder is also an RNN which is initialized with a single context vector $c = h_T$ as its inputs and generates an output sequence (y_1, y_2, \dots, y_N) vector by vector, where N is the length of output sequence. At each time step t , h_t and s_t denote the hidden states of the encoder and decoder respectively. There are two well known challenges with this traditional encoder-decoder framework. First, a critical disadvantage of single context vector design is the incapability of the system to remember long sequences: all the intermediate states of the encoder are discarded and only the final hidden state vector is used to initialize the decoder. This technique works only for small sequences, however, as the length of the sequence increases, the vector becomes a bottleneck and may lead to loss of information [14]. Second, it is unable to capture the need of alignment between input and output sequences, which is an essential aspect of structured output tasks such as machine translation or text summarization [15]. The ‘attention mechanism’, first introduced for machine translation by Bahdanau et al. in [9], was born to address these problems. The novelty in their approach is that they use an alignment function that for each output word finds important input words, thus the neural network learns to align and translate at the same time. The central idea behind the attention is not to discard the intermediate encoder states but to combine and utilize all the states in order to construct the context vectors required by the decoder to generate the output sequence. The mechanism induces attention weights over the input sequence to prioritize the set of positions where relevant information is present for generating the next time step of the target sequence. Following the definition from Bahdanau et al., attention-based models compute a context vector c_t for each time step as the weighted sum of all hidden states of the encoder and their corresponding attention weights are calculated as follows:

$$e_{tj} = a(s_{t-1}, h_j), \quad \alpha_{tj} = \frac{\exp(e_{tj})}{\sum_{k=1}^T \exp(e_{tk})}, \quad c_t = \sum_{j=1}^T \alpha_{tj} h_j,$$

where a is a learned function which can be thought of as computing a scalar importance value for h_j given the value of h_j and the previous state s_{t-1} and each attention weight α_{tj} determines the normalized importance score for h_j . As shown in Figure 1, the context vectors c_t are then used to compute the decoder hidden state sequence, where s_t depends on s_{t-1} , c_t and y_{t-1} . The attention weights can be learned by incorporating an additional feed-forward neural network that is jointly trained with encoder-decoder components of the architecture.

The intuition is that an attention-based model could help in the energy disaggregation task by assigning importance to each position of the aggregated signal which corresponds to

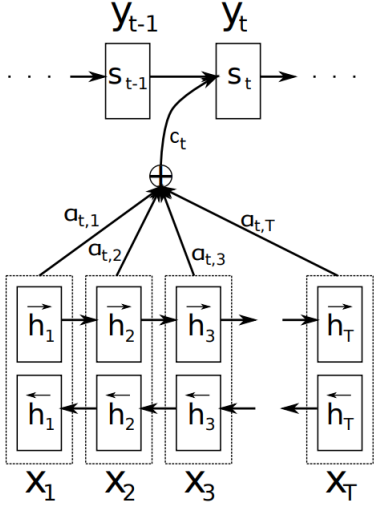


Fig. 1. Original graphical illustration of the proposed model by Bahdanau et al. in [9].

the position of an activation, or more generally, to a state change of the target appliance. This allows the neural network to focus its representational power on selected time steps of the target appliance in the aggregated signal, rather than on the activations of non-target appliances, hopefully yielding more accurate predictions.

In neural machine translation, languages are typically not aligned because of the word ordering between the source and the target language. For the NILM problem, the aggregated power consumption is perfectly aligned with the load of the corresponding appliance and the alignment is known ahead of time. For this reason, to amplify the contribution of an appliance activation in the aggregated signal, we use the simplified attention model inspired by Raffel and Ellis in [16], that aggregates all the hidden states of the encoder using their relative importance. The attention mechanism can be formulated as follows:

$$e_t = a(h_t), \quad \alpha_t = \frac{\exp(e_t)}{\sum_{j=1}^T \exp(e_j)}, \quad c = \sum_{t=1}^T \alpha_t h_t,$$

where a is a learnable function that depends only on the hidden state vector of the encoder h_t . The learnable function can be implemented with a feed-forward network that learns a particular attention weight α_t that determines the normalized importance score for h_j . This allows the network to compare and choose the time steps that are more relevant to the desired output which results in more focused attention value.

B. Network Topology

The novelty of the architecture consists in both the presence of the attention mechanism, and the structure of the decoder, where no recursive neural network is needed. Indeed, the adopted attention mechanism allows one to decouple the input representation from the output and the structure of the encoder from the structure of the decoder. We exploit these benefits and we introduce an innovative hybrid encoder-decoder which is

based on a combination of convolutional layers and recurrent layers for the encoder and fully connected layers followed by convolutional layers for the decoder. More in detail, the network topology proposed here for the NILM is the following:

Encoder: the encoder network is composed by a CNN with two one-dimensional convolutional layers (Conv1D) with linear activation function that process the input aggregated signal (x_1, x_2, \dots, x_T) and produce a set of feature maps. Finally a RNN takes as input the set of feature maps and produces the sequence of the hidden states summarizing all the information of the aggregated signal. We use Bidirectional LSTM (BiLSTM) in order to get the hidden states (h_1, h_2, \dots, h_T) that summarize the information from both directions. A bidirectional LSTM consists of a forward LSTM \vec{f} that reads the sequence from left to right and a backward LSTM \vec{f} that reads it from right to left. We obtain the final sequence of hidden states of the encoder by concatenating the hidden state vectors from both directions, i.e., $h_t = [h_t^f; h_t^b]^T$.

Attention: the attention unit between the encoder and the decoder consists of a single layer feed-forward neural network that computes the attention weights and returns the context vector as a weighted average of the output of the encoder over time. Not all the feature maps produced by the CNN have equal contribution in the identification of the activation of the target appliance. Thus the attention mechanism captures salient activations of the appliance, extracting more valuable feature maps than others for the disaggregation. The implemented attention unit is shown in Figure 2 and it is mathematically defined as follows:

$$e_t = V_a^T \tanh(W_a h_t + b_a),$$

$$\alpha_t = \text{softmax}(e_t),$$

$$c = \sum_{t=1}^T \alpha_t h_t,$$

where V_a , W_a and b_a are the attention parameters jointly learned with the other components of the architecture. The output of the attention unit is the context vector c that is used as the input vector for the following decoder.

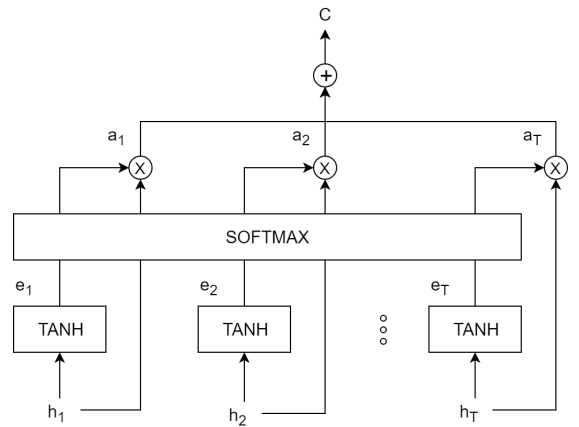


Fig. 2. Graphical illustration of the implemented attention unit.

Decoder: the decoder network is composed of two fully connected layers (Dense) followed by the rectified linear unit

(ReLU) activation function that calculates the maximum between its input and zero, preventing the occurrence of negative values of the disaggregated active power. Finally a CNN structured specularly to the encoder closes the network and outputs the disaggregated signal (y_1, y_2, \dots, y_T) by performing a deconvolution.

The exact architecture is shown in Figure 3, and is defined as follows:

- 1) Input (sequence length L determined by the appliance duration)
- 2) Conv1D (convolutional layer with F filters, $\text{kernel_size}=K$, stride=1, and linear activation function)
- 3) Conv1D (convolutional layer with F filters, $\text{kernel_size}=K$, stride=1, and linear activation function)
- 4) BiLSTM (bidirectional LSTM with H units, returning a sequence of context vectors and tangent hyperbolic activation function)
- 5) Attention (single layer feed-forward neural network with H units, and tangent hyperbolic activation function)
- 6) Dense (fully connected layer with $L \times F$ units, and ReLU activation function)
- 7) Dense (fully connected layer with $L \times F$ units, and ReLU activation function)
- 8) Conv1D (convolutional layer with F filters, $\text{kernel_size}=K$, stride=1, and linear activation function)
- 9) Conv1D (convolutional layer with 1 filter, $\text{kernel_size}=K$, stride=1, and linear activation function)
- 10) Output (sequence length L)

We call our model S2SwA, as the short for Sequence-to-Sequence with Attention.

IV. EXPERIMENTS

In this section we describe the experiments conducted to evaluate the performance of our S2SwA approach. First, we describe the performance metrics, the datasets and the experimental procedure adopted. Then, we present and discuss the obtained results.

A. Metrics

In order to evaluate our NILM approach, we need to define useful metrics that capture specific performance aspects of the algorithm. In NILM literature, performance metrics are generally divided in energy-based metrics and state-based metrics [2]. State-based metrics are related to binary classification metrics and focus on the appliance state detection where the actual and predicted state are estimated using appliance-specific on/off-thresholds. For the appliance i , true positives (TP), false positives (FP), false negatives (FN), and true negatives (TN) are defined as follows:

$$TP_i = \sum_{t=1}^T \mathbb{1}(s_i(t) = \text{on}, \hat{s}_i(t) = \text{on}),$$

$$FP_i = \sum_{t=1}^T \mathbb{1}(s_i(t) = \text{off}, \hat{s}_i(t) = \text{on}),$$

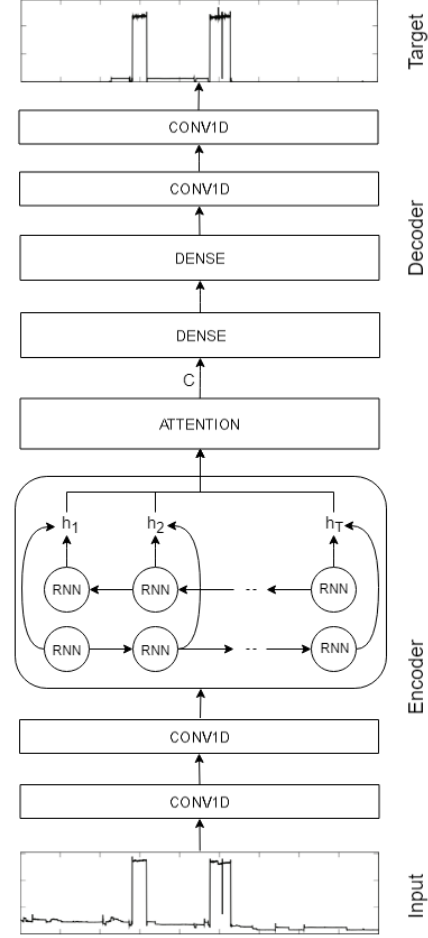


Fig. 3. Encoder-decoder architecture with attention mechanism employed for energy disaggregation.

$$FN_i = \sum_{t=1}^T \mathbb{1}(s_i(t) = \text{on}, \hat{s}_i(t) = \text{off}),$$

$$TN_i = \sum_{t=1}^T \mathbb{1}(s_i(t) = \text{off}, \hat{s}_i(t) = \text{off}),$$

where $\mathbb{1}(\cdot)$ is the boolean predicate function, $s_i(t)$ and $\hat{s}_i(t)$ are respectively the actual and the predicted state of the appliance i at time index t . The state of an appliance is considered ‘on’ when the consumption is greater than some threshold and ‘off’ when the consumption is less or equal the same threshold. The threshold varies with the appliance and it assumes the same value used for extracting the activations [3]. State-based precision, recall and F_1 -score are determined as follows [17]:

$$P_i^S = \frac{TP_i}{TP_i + FP_i}, \quad R_i^S = \frac{TP_i}{TP_i + FN_i}, \quad F_{1i}^S = 2 \frac{P_i^S \cdot R_i^S}{P_i^S + R_i^S}.$$

State-based precision, recall and F_1 -score return a value between 0 and 1 with a higher number indicating better classification performance.

The Matthews Correlation Coefficient (MCC) [17] is used in machine learning as a measure of the quality of binary clas-

sifications. For the appliance i , it is defined by the following formula:

$$MCC_i = \frac{TP_i \cdot TN_i - FP_i \cdot FN_i}{\sqrt{(TP_i + FP_i)(TP_i + FN_i)(TN_i + FP_i)(TN_i + FN_i)}}.$$

It returns a value in $[-1, 1]$. A coefficient of 1 represents a perfect prediction, 0 no better than random prediction and -1 indicates total disagreement between prediction and observation.

State-based metrics don't take into account that the shape of the estimated load should match the shape of the ground truth. Therefore, energy-based precision and recall scores adopted in [8] are based on the correctly estimated amount of energy in each time interval. Energy-based precision measures the amount of power assigned to an appliance that actually belongs to it, whereas the recall measures the part of the power consumption correctly classified. The F_1 score is, as before, the harmonic average of the precision and recall. For the i -th appliance, these quantities are defined as follows:

$$\begin{aligned} P_i^E &= \frac{\sum_{t=1}^T \min(\hat{y}_i(t), y_i(t))}{\sum_{t=1}^T \hat{y}_i(t)}, \\ R_i^E &= \frac{\sum_{t=1}^T \min(\hat{y}_i(t), y_i(t))}{\sum_{t=1}^T y_i(t)}, \\ F_{1i}^E &= 2 \frac{P_i^E \cdot R_i^E}{P_i^E + R_i^E}, \end{aligned}$$

where $\hat{y}_i(t)$ is the disaggregated power consumption, $y_i(t)$ is the ground truth appliance power consumption, and T is the total number of samples. Energy-based precision, recall and F_1 -score return a value between 0 and 1 with a higher number indicating better performance.

Finally, the Normalized Error in Assigned Power (NEP) [17], measures the deviation of the estimated power from the true power divided by the total energy consumption of the appliance. For the appliance i , NEP is calculated as follows:

$$NEP_i = \frac{\sum_{t=1}^T |y_i(t) - \hat{y}_i(t)|}{\sum_{t=1}^T y_i(t)}.$$

For this metric, lower values indicate better disaggregation performance.

B. Datasets

Following [7], in order to evaluate our algorithm on different scenarios and on data with different granularity, we choose two publicly available datasets. The Alamanac of Minutely Power dataset (AMPds) [12] contains recording of the consumption profiles of a single home in Canada for two years, at 1 minute sampling period. We conduct our experiments by using six appliances: dishwasher (DW), dryer (DR), electric oven (EO), fridge (FR), heat pump (HP) and washing machine (WM). The second dataset, The Domestic Appliance-Level Electricity dataset UK-DALE [4], consists of consumption profiles recorded in five houses in UK over two years, at 6 second sampling period. Here, the experiments are conducted by using five appliances: dishwasher (DW), fridge

(FR), kettle (KE), microwave (MW) and washing machine (WM). In order to perform a fair comparison between our approach and the state-of-the-art, that is the DAE method proposed in [7], we adopt exactly the same experimental setup, i.e. for each dataset we use the same pre-processing, artificial data augmentation approach, and data partitioning into train and test data as described in [7]. More in detail, each dataset is split in different portions for training and testing as specified in Table I, and their dimensions depend on the availability of appliances activation within the dataset. These operations are performed by using NILMTK [17], a toolkit that provides methods for the extraction of the activations from the ground truth power consumption related to each appliance in a dataset. For both datasets, the chosen appliances represent the principal contributions to the peak of power consumption in the aggregated load. This allows us to perform the experiments by focusing only on the noised scenario, since the denoised scenario is a good approximation of the noised one in the regions where the power consumption is higher. The experiments are conducted in seen scenario for the AMPds dataset and in both seen and unseen scenario for the UK-DALE dataset due to the availability of data relative to more than one building. In the *seen* scenario, the model is trained using the training set of a given house and then tested on the test set of the house itself, i.e. in a period that does not belong to the training data. On the other hand, in the *unseen* scenario, the disaggregation is evaluated on the test set related to a house not used in the training phase. For the unseen scenario, the specific houses used for training and testing are shown in Table II.

Dataset	House	Train	Test
AMPds	1	1 year, 6 months	6 months
	1	1 year, 8 months, 3 days	7 days
	2	4 months, 3 days	7 days
	4	6 months, 25 days	7 days
	5	2 months, 3 days	6 days

TABLE I
DEFINITION OF THE TRAINING AND TEST SETS DIMENSION FOR THE
CONSIDERED DATASET IN BOTH SEEN AND UNSEEN SCENARIO.

Appliance	Train	Test
Kettle	1, 2, 4	5
Fridge	1, 2, 4	5
Washing machine	1, 5	2
Microwave	1, 2	5
Dishwasher	1, 2	5

TABLE II
UK-DALE HOUSES USED FOR TRAINING AND TESTING IN THE UNSEEN
SCENARIO.

C. Network Setup

According to the neural NILM approach, we train one network per target appliance. Each network receives data in a mini-batch of 128 examples, and mean and variance standardization is computed on the input data. For the target data, min-max normalization is performed using the minimum and the maximum power consumption values of the related appliance in the training data. The training phase is carried

out with a sliding window technique over the aggregated signal, using overlapped windows with hop size equal to one sample. As stated in [3], the sliding window that selects input and output pairs needs to be large enough to comprise an entire activation of the appliance, but not too large to include other contributions. In Table III we report the adopted window length for each appliance that depends on the sampling rate of the dataset. Each network is trained with the Stochastic Gradient Descent (SGD) algorithm with Nesterov momentum [18] set to 0.9 to minimize the Mean Squared Error (MSE) between its output and the ground truth of a single appliance. The maximum number of epochs is set to 1e4, the initial learning rate is set to 1e-2 and it is reduced by a decay factor equal to 1e-6 as the training progresses. Early stopping is employed as a form of regularization to avoid overfitting since it stops the training as soon as the error on the validation set starts to grow [19]. The hyperparameter optimization regards the number of filters (F), the size of each kernel (K) and the number of neurons in the recurrent layer (H). Grid search is used to perform hyperparameter optimization, which is simply an exhaustive search through a manually specified subset of points in the hyperparameter space of the neural network where $F=\{2, 4, 8, 16, 32\}$, $K=\{2, 4, 8, 16, 32\}$ and $H=\{64, 128, 256, 512, 1024\}$. We evaluate the configuration of the hyperparameters on a held-out validation set and we choose the architecture that achieves the highest performance on it. The disaggregation phase, also carried out with a sliding window over the aggregated signal with hop size equal to one sample, generates overlapped windows of the disaggregated signal. Differently from what proposed in [3], where the authors recompose the overlapped windows by aggregating their mean value, we adopt the strategy proposed in [7] in which the disaggregated signal is recombined by using a median filter on the overlapped portions. The neural networks are implemented in Python with PyTorch, an open source machine learning framework [20] and the experiments are conducted on cluster of NVIDIA Tesla K80 GPUs. The training time requires several hours for each architecture depending on the network dimension and on the granularity of the dataset.

Dataset	DW	DR	EO	FR	HP	KE	MW	WM
AMPds	210	75	120	45	90	-	-	120
UK-DALE	1536	-	-	512	-	128	288	1024

TABLE III

WINDOW LENGTH (L) FOR THE S2SwA ARCHITECTURE FOR THE DIFFERENT APPLIANCES.

D. Results

For the AMPds dataset, the S2SwA algorithm outperforms the DAE across all the appliances, as shown in Table IV. More in detail, for the F1 energy and F1 state metrics, there is an overall improvement of 25.95% and 22.64% respectively. The same overall behaviour can be observed for all the other metrics. Analyzing the performance of the individual appliances, the S2SwA algorithm achieves superior performance for all the appliances and best improvement in terms of the considered metrics can be observed for the heat pump and

the dishwasher. Indeed, for the electric oven and the dryer the performance improvement is modest compared to the other appliances. The profiles related to the dishwasher and the electric oven are shown in Figure 4 and Figure 5 where each appliance activation is correctly detected by the S2SwA in the disaggregated trace.

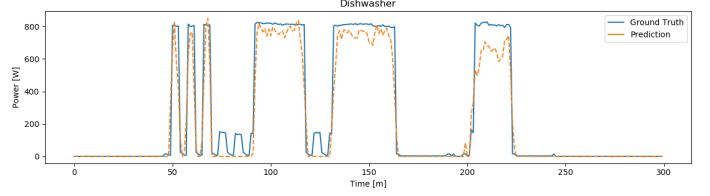


Fig. 4. Ground truth and disaggregated profiles related to the dishwasher of the AMPds dataset.

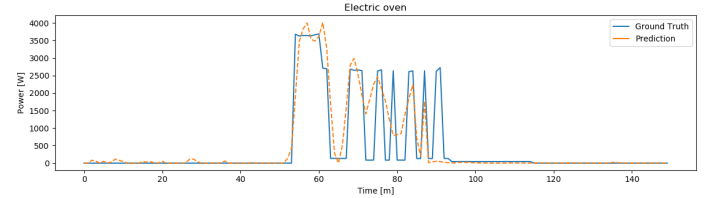


Fig. 5. Ground truth and disaggregated profiles related to the electric oven of the AMPds dataset.

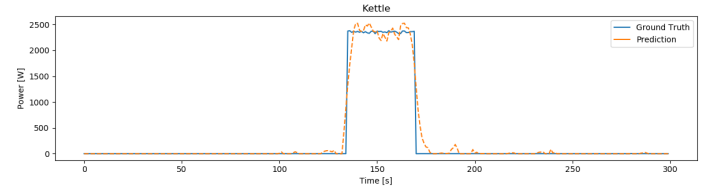


Fig. 6. Ground truth and disaggregated profiles related to the kettle of the UK-DALE dataset, seen scenario.

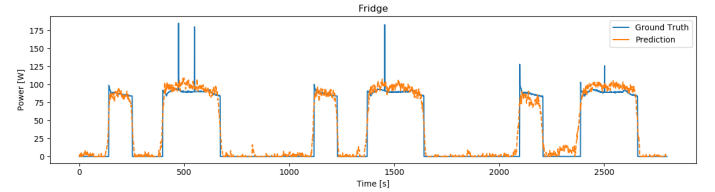


Fig. 7. Ground truth and disaggregated profiles related to the fridge of the UK-DALE dataset, seen scenario.

Considering the UK-DALE experiments in seen scenario, the profiles related to the kettle and fridge in the house 1 are shown in Figure 6 and Figure 7. The appliance activation is correctly detected without producing false positives in the disaggregated trace. In this case the S2SwA algorithm outperforms the DAE across all the appliances as shown in Table V. More in detail, the washing machine and the fridge report the biggest improvement for all the considered metrics with respect to the DAE. For the remaining appliances, the

performance improvement is modest. As stated before, the availability of more than one building in the UK-DALE dataset allows us to evaluate the algorithm on an unseen scenario. The results in Table VI show that the our proposed method outperforms the DAE method in the average across all the appliances. The generalization property of the S2SwA approach allows to apply the model on a building not seen during the training, with a reasonable degradation of performance. This is a desirable property in a NILM algorithm since the unseen scenario represents the real world application of the NILM service.

Modeling attention is particularly interesting from the perspective of the interpretability of deep learning models because it allows to directly inspect the internal working of the architecture. The hypothesis is that the magnitude of the attention weights correlates with how relevant the specific region of the input sequence is, for the prediction of the output sequence. As shown in Figure 8 and Figure 9, our network is effective at predicting the activation of an appliance and the attention weights present a peak in correspondence of the state change of that appliance.

In conclusion, our approach does not only predict the correct disaggregation in terms of scale, but is also successful at deciding if the target appliance is active in the aggregate load at a given time step.

Net	Metric	DW	DR	EO	FR	HP	WM	Overall
DAE [7]	F_1^E	0.498	0.912	0.573	0.391	0.654	0.119	0.524
	NEP	0.640	0.131	0.568	0.940	0.419	4.416	1.185
	F_1^S	0.582	0.768	0.459	0.331	0.798	0.108	0.508
	MCC	0.593	0.784	0.489	0.217	0.789	0.165	0.506
S2SwA	F_1^E	0.724	0.956	0.596	0.482	0.911	0.292	0.660
	NEP	0.483	0.089	0.504	0.749	0.172	2.668	0.777
	F_1^S	0.706	0.972	0.492	0.388	0.930	0.250	0.623
	MCC	0.726	0.973	0.490	0.379	0.924	0.263	0.626

TABLE IV

DISAGGREGATION PERFORMANCE FOR THE AMPDs DATASET. IN BOLD THE BEST PERFORMING APPROACH.

Net	Metric	DW	FR	KE	MW	WM	Overall
DAE [7]	F_1^E	0.843	0.736	0.824	0.724	0.548	0.735
	NEP	0.278	0.472	0.393	0.524	2.135	0.760
	F_1^S	0.556	0.782	0.866	0.755	0.408	0.673
	MCC	0.583	0.683	0.866	0.751	0.425	0.661
S2SwA	F_1^E	0.897	0.796	0.829	0.759	0.711	0.798
	NEP	0.199	0.419	0.329	0.478	0.601	0.405
	F_1^S	0.698	0.858	0.882	0.770	0.721	0.785
	MCC	0.701	0.741	0.883	0.777	0.730	0.766

TABLE V

DISAGGREGATION PERFORMANCE IN THE SEEN SCENARIO FOR THE UK-DALE DATASET. IN BOLD THE BEST PERFORMING APPROACH.

Net	Metric	DW	FR	KE	MW	WM	Overall
DAE [7]	F_1^E	0.692	0.787	0.836	0.458	0.535	0.666
	NEP	0.648	0.419	0.177	1.383	1.439	0.813
	F_1^S	0.509	0.828	0.956	0.454	0.675	0.684
	MCC	0.502	0.757	0.957	0.510	0.687	0.683
S2SwA	F_1^E	0.739	0.785	0.854	0.549	0.603	0.706
	NEP	0.534	0.399	0.098	0.951	0.896	0.576
	F_1^S	0.608	0.824	0.967	0.585	0.701	0.737
	MCC	0.622	0.787	0.973	0.523	0.693	0.719

TABLE VI

DISAGGREGATION PERFORMANCE IN THE UNSEEN SCENARIO FOR THE UK-DALE DATASET. IN BOLD THE BEST PERFORMING APPROACH.

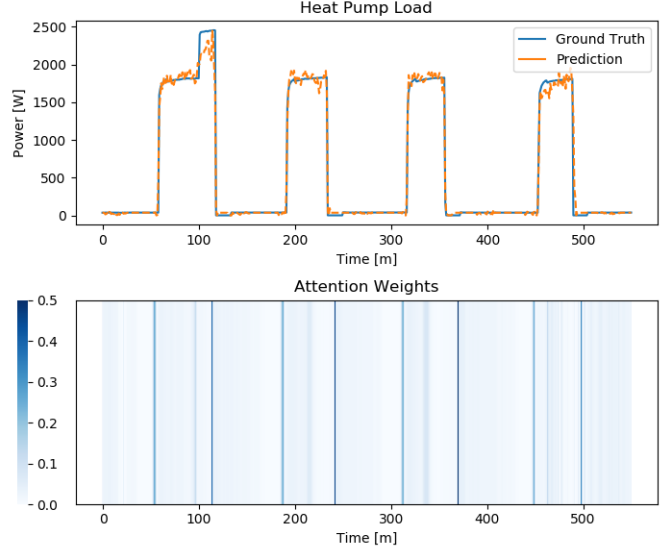


Fig. 8. Heat pump load profiles and the correspondent heatmap of the attention weights in the considered time slot.

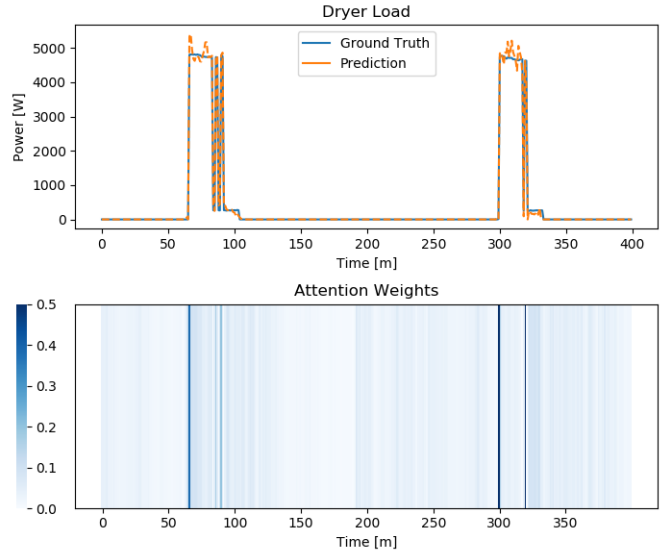


Fig. 9. Dryer load profiles and the correspondent heatmap of the attention weights in the considered time slot.

V. CONCLUSIONS

This paper proposes a new deep neural network architecture for the NILM problem that integrates a tailored attention mechanism with the encoder-decoder framework to extract appliance specific power usage from the aggregated signal. The integration of convolutional layers and recurrent layers facilitates feature extraction, and allows to build more generalized appliance models where the locations of relevant features are successfully identified by the attention mechanism. The proposed system is trained on two real-world datasets with different granularity, AMPDs and UK-DALE, in seen and unseen conditions. The performance is evaluated by using both energy-based and state-based metrics: the first, evaluate the capability of the algorithm to estimate the actual power profile

of the appliances, while the second measure the capability of identifying whether the appliance is in the ‘on’ or ‘off’ state. The experimental results demonstrate that the proposed model outperforms the DAE initially proposed by Kelly and Knottenbely in [3] and later improved by Bonfigli et al. in [7] in all the addressed experimental conditions. The proposed model remarkably improves accuracy and generalization capability for load recognition for both datasets compared to the deep learning state-of-the-art. Since the experimental setting is identical to the one used in [7], it is clear that the improvement is due to the new architecture.

REFERENCES

- [1] G. W. Hart, “Nonintrusive appliance load monitoring,” *Proceedings of the IEEE*, vol. 80, no. 12, pp. 1870–1891, Dec 1992.
- [2] A. Faustine, N. H. Mvungi, S. Kajage, and K. Michael, “A survey on non-intrusive load monitoring methodologies and techniques for energy disaggregation problem,” *arXiv preprint arXiv:1703.00785*, 2017.
- [3] J. Kelly and W. Knottenbelt, “Neural nilm: Deep neural networks applied to energy disaggregation,” in *Proceedings of the 2nd ACM International Conference on Embedded Systems for Energy-Efficient Built Environments*. ACM, 2015, pp. 55–64.
- [4] ———, “The uk-dale dataset, domestic appliance-level electricity demand and whole-house demand from five uk homes,” *Scientific data*, vol. 2, p. 150007, 2015.
- [5] W. He and Y. Chai, “An empirical study on energy disaggregation via deep learning,” in *2016 2nd International Conference on Artificial Intelligence and Industrial Engineering (AIE 2016)*. Atlantis Press, 2016.
- [6] C. Zhang, M. Zhong, Z. Wang, N. Goddard, and C. Sutton, “Sequence-to-point learning with neural networks for non-intrusive load monitoring,” in *Thirty-Second AAAI Conference on Artificial Intelligence*, 2018.
- [7] R. Bonfigli, A. Felicetti, E. Principi, M. Fagiani, S. Squartini, and F. Piazza, “Denoising autoencoders for non-intrusive load monitoring: improvements and comparative evaluation,” *Energy and Buildings*, vol. 158, pp. 1461–1474, 2018.
- [8] J. Z. Kolter and T. Jaakkola, “Approximate inference in additive factorial hmms with application to energy disaggregation,” in *Artificial Intelligence and Statistics*, 2012, pp. 1472–1482.
- [9] D. Bahdanau, K. Cho, and Y. Bengio, “Neural machine translation by jointly learning to align and translate,” *arXiv preprint arXiv:1409.0473*, 2014.
- [10] Q. You, H. Jin, Z. Wang, C. Fang, and J. Luo, “Image captioning with semantic attention,” in *Proceedings of the IEEE conference on computer vision and pattern recognition*, 2016, pp. 4651–4659.
- [11] W. Chan, N. Jaitly, Q. V. Le, and O. Vinyals, “Listen, attend and spell,” *arXiv preprint arXiv:1508.01211*, 2015.
- [12] S. Makonin, F. Popowich, L. Bartram, B. Gill, and I. V. Bajić, “Ampds: A public dataset for load disaggregation and eco-feedback research,” in *2013 IEEE Electrical Power & Energy Conference*. IEEE, 2013, pp. 1–6.
- [13] I. Sutskever, O. Vinyals, and Q. V. Le, “Sequence to sequence learning with neural networks,” in *Advances in neural information processing systems*, 2014, pp. 3104–3112.
- [14] K. Cho, B. Van Merriënboer, D. Bahdanau, and Y. Bengio, “On the properties of neural machine translation: Encoder-decoder approaches,” *arXiv preprint arXiv:1409.1259*, 2014.
- [15] T. Young, D. Hazarika, S. Poria, and E. Cambria, “Recent trends in deep learning based natural language processing,” *ieee Computational intelligence magazine*, vol. 13, no. 3, pp. 55–75, 2018.
- [16] C. Raffel and D. P. Ellis, “Feed-forward networks with attention can solve some long-term memory problems,” *arXiv preprint arXiv:1512.08756*, 2015.
- [17] N. Batra, J. Kelly, O. Parson, H. Dutta, W. Knottenbelt, A. Rogers, A. Singh, and M. Srivastava, “Nilmtk: an open source toolkit for non-intrusive load monitoring,” in *Proceedings of the 5th international conference on Future energy systems*. ACM, 2014, pp. 265–276.
- [18] I. Sutskever, J. Martens, G. Dahl, and G. Hinton, “On the importance of initialization and momentum in deep learning,” in *International conference on machine learning*, 2013, pp. 1139–1147.
- [19] R. Caruana, S. Lawrence, and L. Giles, “Overfitting in neural nets: Backpropagation, conjugate gradient, and early stopping,” in *Proceedings of the 13th International Conference on Neural Information Processing Systems*, ser. NIPS’00. MIT Press, 2000, pp. 381–387.
- [20] A. Paszke, S. Gross, S. Chintala, G. Chanan, E. Yang, Z. DeVito, Z. Lin, A. Desmaison, L. Antiga, and A. Lerer, “Automatic differentiation in PyTorch,” in *NIPS Autodiff Workshop*, 2017.